

THE PHYSICAL REVIEW

A journal of experimental and theoretical physics established by E. L. Nichols in 1893

SECOND SERIES VOL. 103, No. 5

SEPTEMBER 1, 1956

Oscillations of Liquid Helium in a U-Tube*†‡

R. J. DONNELLY, *Sloane Physics Laboratory, Yale University, New Haven, Connecticut*

AND

O. PENROSE, *Sterling Chemistry Laboratory, Yale University, New Haven, Connecticut*

(Received May 11, 1956)

Frictional forces in He II were studied by observing the decay of free oscillations in a U-tube. The decay, unlike that for ordinary liquids (including He I), is characterized by *two* logarithmic decrements: one for amplitudes of oscillation below about 0.1 cm, and another for amplitudes between about 0.2 and 1 cm. The values of these two decrements agree with the results of a hydrodynamical calculation which assumes that for the lower range of amplitudes the two-fluid equations of Landau and Tisza hold, and that for the other range of amplitudes the normal and superfluid components have identical velocity fields. The values for the viscosity coefficient deduced from the observations agree roughly with each other and with the published results of other methods. Despite the large experimental error, there is evidence that the viscosity when the two components move together is higher than the viscosity of the normal component when the two-fluid equations hold, the ratio being about 1.33:1.

The transition between the two types of behavior is fairly sharp near the lambda point but becomes diffuse as the temperature is lowered to 1°K. At a given temperature, the transition appears to be sharper the more gentle the bend of the U-tube, that is, the more uniform the velocity over the walls of the tube.

1. INTRODUCTION

HYDRODYNAMICAL experiments with liquid helium II have shown that the two-fluid hydrodynamical equations proposed by Landau¹ and Tisza^{2,3} have only a limited range of validity. Although these equations account for the frictionless flow of He II in slits⁴ and for the results of Andronikashvili's experiment with a pile of disks⁵ when the velocities involved are small enough, they fail to account for the additional frictional effects observed in both experiments^{4,6} at larger velocities. They also fail to account for the shape

of the meniscus in a rotating vessel containing He II^{7,8}; in fact, the observations in this experiment are most easily explained by assuming that the normal and superfluid components move together. It appears, therefore, that for small enough velocities the two-fluid equations of Landau and Tisza hold, but for larger velocities some frictional force acts tending to make the two fluids move together.

Benson and Hollis Hallett⁹ have studied these effects by observing the torsional oscillations of a sphere suspended in liquid helium by a fiber. They observed that the damping of the oscillations depended upon amplitude, as sketched in Fig. 1(a). Between the lambda point and about 2°K, there are two distinct amplitude ranges within which the damping is independent of amplitude. In the low-amplitude range, the observed damping agrees with the predictions of the two-fluid equations (that is, with the assumption that only the normal fluid is dragged by the moving sphere);

* Supported by the Office of Ordnance Research of the U. S. Army and by the National Science Foundation.

† Contribution No. 1359 from the Sterling Chemistry Laboratory.

‡ This paper formed part of a dissertation presented to Yale University by R. J. Donnelly in 1956 for the degree of Doctor of Philosophy.

¹ L. D. Landau, *J. Phys. (U.S.S.R.)* **5**, 71 (1941).

² L. Tisza, *Phys. Rev.* **72**, 838 (1947).

³ F. London, *Superfluids* (John Wiley and Sons, Inc., New York, 1954), Vol. 2, pp. 83–87, 126–137.

⁴ J. F. Allen and A. D. Misener, *Proc. Roy. Soc. (London)* **A172**, 467 (1939).

⁵ E. L. Andronikashvili, *J. Phys. (U.S.S.R.)* **10**, 201 (1946); *Zhur. Eksp'l. i Teort. Fiz.* **18**, 424, 429 (1948).

⁶ A. C. Hollis Hallett, *Proc. Roy. Soc. (London)* **A210**, 404 (1952).

⁷ D. V. Osborne, *Proc. Phys. Soc. (London)* **A63**, 909 (1950).

⁸ Donnelly, Chester, Walmsley, and Lane, *Phys. Rev.* **102**, 3 (1956).

⁹ C. B. Benson and A. C. Hollis Hallett, *Conférence de Physique des Basses Températures* (Union Internationale de Physique Pure et Appliquée, Paris, 1955), p. 73.

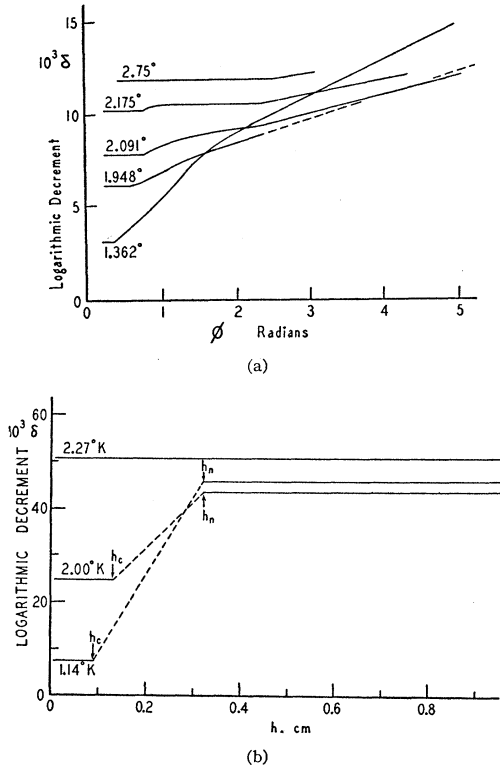


FIG. 1. (a) Logarithmic decrement, δ , as a function of amplitude, ϕ , for the oscillating sphere experiment (after Benson and Hollis Hallett⁹). (b) Logarithmic decrement, δ , as a function of amplitude, h , for the U-tube experiment. This figure was prepared from the data given in Table I.

in the other range, however, it indicates that both normal and superfluid components are dragged. Thus two distinct types of hydrodynamical behavior are demonstrated in a single experiment.

In Benson and Hallett's experiment the transition between the two types of behavior becomes diffuse as the temperature is reduced, and the higher-amplitude range is ill-defined below 2°K. The reason for this may be that the velocity is not uniform over the surface of the sphere, but varies from zero at the poles to a maximum at the equator. If this is so, an experiment where the velocity is roughly uniform over the oscillating surface might show a sharper transition.

With the object of demonstrating more clearly the effects observed by Benson and Hallett, we have studied the damping of free oscillations of a column of liquid helium in a U-tube. The variation of damping with amplitude is sketched in Fig. 1(b). As in Benson and Hallett's experiment, there are two distinct amplitude ranges, but now, perhaps for the reason mentioned above, the transition remains fairly abrupt down to 1°K.

In the next section we shall calculate the relation between the viscosity and the damping of the oscillations in two ways: (i) assuming that the two-fluid equations hold, and (ii) assuming that the two fluids

move together at all times. Comparison with the experimental results will then show that reasonable values for the viscosity are obtained by using assumption (i) for the low-amplitude range and (ii) for the other range.

2. THEORY

We first calculate the logarithmic decrement of the oscillations according to the two-fluid equations. To simplify the problem, we make the following assumptions:

- (i) The motion is laminar.
- (ii) ρ_n , ρ_s , and the entropy density can be treated as constant.
- (iii) Effects due to the bend and ends are negligible.

The equations of conservation of mass and entropy are, respectively,^{1,3}

$$\begin{aligned}\dot{\rho}_n + \dot{\rho}_s &= -\text{div}(\rho_n \mathbf{v}_n + \rho_s \mathbf{v}_s), \\ \dot{\sigma} &= -\text{div}(\sigma \mathbf{v}_n),\end{aligned}$$

where σ is the entropy density, and the other symbols have their usual meanings. By virtue of assumption (ii), these equations simplify to

$$\text{div} \mathbf{v}_n = \text{div} \mathbf{v}_s = 0. \quad (1)$$

It follows from Gauss' theorem that the surface integrals $\int_S \mathbf{v}_n \cdot d\mathbf{S}$ and $\int_S \mathbf{v}_s \cdot d\mathbf{S}$, where S is any cross section of the tube, are independent of the position of S . Each of these expressions can therefore be equated to its value just below the meniscus in one arm of the U-tube. We have therefore, for any S , provided a suitable sign convention is used,

$$\pi a^2 \dot{h} = \int_S \mathbf{v}_n \cdot d\mathbf{S} = \int_S \mathbf{v}_s \cdot d\mathbf{S}, \quad (2)$$

where h is the height of the meniscus in question above its equilibrium level, and a is the radius of the tube.

Before trying to solve the hydrodynamical equations of motion, we use assumption (iii) to simplify the geometry. That is, we assume that the velocity profile in a U-tube is the same as in an infinitely long cylindrical tube of the same radius, with a uniform pressure gradient equal to the average pressure gradient in the liquid—that is, to $2\rho g h/l$, where g is the acceleration of gravity and l is the length of the liquid column. By assumption (i), we may take \mathbf{v}_n and \mathbf{v}_s to lie along the axis of the cylinder and to depend on the radial coordinate r only. This automatically satisfies Eq. (1). The equation of momentum conservation¹ can now be written

$$\rho_n \dot{v}_n + \rho_s \dot{v}_s = -2\rho g h/l + \eta(\partial^2/\partial r^2 + r^{-1}\partial/\partial r)v_n, \quad (3)$$

where v_n and v_s are the axial components of the vectors \mathbf{v}_n and \mathbf{v}_s , and η is the viscosity of the normal component.

The equation of motion of the superfluid leads^{1,3} to the condition

$$\text{curl} \mathbf{v}_s = 0. \quad (4)$$

This implies here that v_s is independent of r . Thus we can rewrite Eq. (2) as follows:

$$\dot{h} = v_s \quad (5a)$$

$$= 2a^{-2} \int_0^a v_n(r) r dr. \quad (5b)$$

To find the period and damping of sinusoidal oscillations, we seek a solution of Eqs. (3) and (5) in the form

$$\begin{aligned} v_n &= \text{Rl}V(r)e^{i\omega t}, \\ h &= \text{Rl}He^{i\omega t}, \end{aligned} \quad (6)$$

where V , H , and ω are complex quantities, and Rl stands for "real part of." Using (5a) to eliminate v_s from (3), and substituting (6) into the resulting equation and also into (5b), we obtain

$$(\partial^2/\partial r^2 + r^{-1}\partial/\partial r - i\omega\rho_n\eta^{-1})V = (\omega_0^2\rho - \omega^2\rho_s)\eta^{-1}H, \quad (7)$$

and

$$i\omega H = 2a^{-2} \int_0^a V(r) r dr, \quad (8)$$

where $\omega_0 \equiv (2g/l)^{1/2}$ is the angular frequency for zero viscosity.

The boundary conditions on v_n are that it should vanish at the surface of the tube (that is, when $r=a$) and should be finite when $r=0$. Accordingly V satisfies the same boundary conditions. Introducing the new symbols

$$y \equiv r(\omega\rho_n/i\eta)^{1/2}, \quad (9a)$$

$$z \equiv a(\omega\rho_n/i\eta)^{1/2}, \quad (9b)$$

where $i^{1/2} \equiv e^{1/2\pi i}$, we find that the appropriate solution of (7) is

$$V = H(\omega^2\rho_s - \omega_0^2\rho)(i\omega\rho_n)^{-1} [1 - J_0(y)/J_0(z)], \quad (10)$$

where J_0 is the zero-order Bessel function. To determine ω , we eliminate V and H from (8) and (10):

$$i\omega = 2(\omega^2\rho_s - \omega_0^2\rho)(i\omega\rho_n a^2)^{-1} \int_0^a [1 - J_0(y)/J_0(z)] r dr.$$

Multiplying both sides by $-i\omega\rho_n/(\omega_0^2\rho - \omega^2\rho_s)$ and subtracting the identity $1 = 2a^{-2} \int_0^a r dr$, we obtain

$$(\omega_0^2 - \omega^2)\rho/(\omega_0^2\rho - \omega^2\rho_s) = 2[a^2 J_0(z)]^{-1} \int_0^a J_0(y) r dr,$$

which reduces to

$$(\omega_0^2 - \omega^2)\rho/(\omega_0^2\rho - \omega^2\rho_s) = 2J_1(z)/zJ_0(z), \quad (11)$$

since $d[yJ_1(y)]/dy = yJ_0(y)$ and $rdr/a^2 = ydy/z^2$.

To find ω , we must solve the simultaneous equations (9b) and (11). A useful approximate solution is given by the assumptions that $\omega \simeq \omega_0$ and that the quantity

$$\lambda \equiv a^{-1}(i\eta/\omega_0\rho_n)^{1/2} \quad (12)$$

is small. Then (9b) becomes $z \simeq \lambda^{-1}$. It follows that $\text{Im}z$ is large and negative, so that the asymptotic formula for $J_n(z)$ becomes

$$J_n(z) \sim \frac{1}{2}(2/\pi z)^{1/2} \exp[i(z - \frac{1}{2}n\pi - \frac{1}{4}\pi)].$$

This implies $J_1(z)/J_0(z) \sim -i$, so that (11) becomes

$$(\omega_0^2 - \omega^2)\rho/(\omega_0^2\rho - \omega^2\rho_s) \simeq -2i\lambda,$$

and ω is approximately given by

$$\omega \simeq \omega_0(1 + 2i\lambda)^{1/2}(1 + 2i\lambda\rho_s/\rho)^{-1/2} \simeq \omega_0(1 + i\lambda\rho_n/\rho). \quad (13)$$

The logarithmic decrement δ is given in terms of ω by

$$\delta = 2\pi(\text{Im}\omega)/(\text{Rl}\omega). \quad (14)$$

Substituting from (13) and using (12) we obtain the result $\delta \simeq \pi\sqrt{2}|\lambda|\rho_n/\rho$ from which it follows, with the help of (12), that

$$\eta = \omega_0\rho_n a^2 |\lambda|^2 \simeq \omega_0 a^2 \delta^2 \rho^2 / 2\pi^2 \rho_n. \quad (15)$$

More accurate methods of determining ω and δ are discussed in the appendix. It is shown there that, provided $\eta/\rho a^2 \omega_0$ is negligible (in our experiment it was roughly 10^{-4}) a good approximation for η is

$$\eta \simeq \frac{a^2 \delta^2 \rho^2}{\pi P \rho_n} \left[1 + \frac{3\delta}{2\pi} - F\left(\frac{\rho\delta}{\rho_n}\right) \right], \quad (16)$$

where P is the measured period of oscillation, and F is a correction given graphically in Fig. 7. For small values of $\rho\delta/\rho_n$ it has the form

$$F = 3\rho\delta/\pi\rho_n + O(\rho\delta/\rho_n)^2. \quad (17)$$

The above calculation refers to the case when the two-fluid equations are valid. However, we can obtain the corresponding results for two other cases without further calculation: (i) An ordinary fluid (e.g., He I). This is merely a special case of the above calculation, with $\rho_s = 0$, $\rho_n = \rho$, and η the viscosity. (ii) He II when frictional forces act between the normal and superfluid components. We assume that the frictional forces, in effect, prevent all relative motion of the two fluids. In other words, we abandon Eq. (4), replacing it by

$$\mathbf{v}_s = \mathbf{v}_n, \quad (18)$$

and we retain Eq. (3) unchanged in form, though possibly with a different value for η . Substituting (18) into (3), we see that the problem is now exactly the same as for an ordinary fluid. Thus the relation between δ and η is again found by formally setting $\rho_s = 0$, $\rho_n = \rho$ in Eq. (16). It should be emphasized, however, that this does not mean that ρ_s is actually zero; although the frictional force is great enough to make the He II

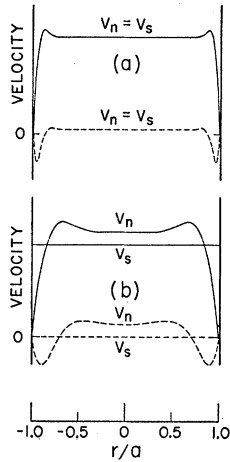


FIG. 2. Typical velocity distributions along a diameter of the U-tube: (a) when the two fluids move together; (b) when the two-fluid equations apply. The curves are calculated for the following combinations of values of the parameters: $a^2\omega_0\rho/\eta=800$, $\rho_n/\rho=\frac{1}{2}$. In the experiment, $a^2\omega_0\rho/\eta$ was roughly 10^4 ; the value 800 exaggerates the thickness of the "boundary layer." The solid curves represent the component in phase with h and the dashed curves the component in quadrature. The values given for v_n are proportional to the real and imaginary parts of $(1+2i^{\frac{1}{2}}x^{-1}) \times [1 - J_0(i^{\frac{1}{2}}x/a)/J_0(i^{\frac{1}{2}}x)]$, with $x \equiv |\lambda|^{-1} = 20\sqrt{2}$ in case (a), and $x = 10$ in case (b).

behave like an ordinary fluid under the present conditions, relative motion of the two fluids would still occur if the conditions were more complicated, e.g., if second sound were superimposed upon the motion considered here. This situation also arises in the rotating bucket experiment, where the He II behaves hydrodynamically like an ordinary fluid^{7,8} but can still propagate second sound.¹⁰

To illustrate the hydrodynamical process which brings about the damping, we have plotted in Fig. 2 typical velocity distributions across a diameter of the tube. The walls of the tube affect the velocity distribution mostly in a narrow "boundary layer," whose thickness in our experiment has the order of magnitude 10^{-2} cm when the two fluids move together [case (a)]. When the two-fluid equations hold [case (b)], this boundary layer is thicker and exists in the normal fluid only, while the velocity distribution of the superfluid is uniform since the superfluid moves irrotationally [see Eq. (4)]. In this case, no frictional forces act directly on the superfluid component; the damping effect of viscosity is transmitted to it indirectly by means of the thermomechanical term, proportional to $\text{grad}T$, in the equation of motion of the superfluid.

It remains to discuss some of the effects due to the bend and ends ignored in the above work. Of these, the only one amenable to numerical estimation is the additional damping caused by the vapor in the tube above the liquid. Applying Poiseuille's law to the flow of this gas, we have estimated the logarithmic decrement arising from this cause to be roughly 5×10^{-5} and therefore negligible. Another source of end effects is surface tension. Since helium wets the walls of the tube, one might expect surface tension forces in the two arms to balance out; however, preliminary tests with water and liquid air indicated a tendency for a thick film of liquid to form on the wall as the liquid level falls and to drain off as the level rises again. This made the damping exceed the theoretical prediction, espe-

cially at large amplitudes. Fortunately, the effect was not visible with liquid helium but it may account for the large experimental scatter. A third complicating factor is the bend of the U-tube. Although a reliable estimate is difficult, intuition suggests that this effect will lead to additional damping, because the flow is more complicated near the bend than in the infinite cylindrical tube considered in the theory.

3. THE EXPERIMENT

Open-ended U-tubes (Fig. 3) were used for the experiment. Although tubes with closed ends would have eliminated the correction for loss of liquid through the film, described below, they would have made necessary much more difficult corrections for the compressibility of the vapor and for evaporation and recondensation. The U-tubes were made of Pyrex and had fairly uniform diameter, even at the bends. The U-tube was supported inside the cryostat at one end of a $\frac{3}{16}$ -in. stainless steel rod; the other end of the rod projected, through a rubber O-ring seal, out of the cryostat and was used to raise and lower the U-tube. A cylindrical plunger about 5 cm long, fitting loosely into one arm of the U-tube, was suspended and controlled in the same way.

For each run, the U-tube was immersed in the liquid helium bath and then raised until about 3 cm of the tube was above the bath. The plunger was then inserted into one arm of the tube. As soon as the temperature, determined by measuring the pressure of the helium vapor with an oil manometer, was steady, the oscillations were started by withdrawing the plunger. The liquid level in one arm of the tube was observed using a cathetometer with a reticule eyepiece. The highest level attained in each complete period of oscillation was observed; every time this maximum level corresponded to a ruling of the reticule the time was recorded. Observations were continued for some minutes after the oscillations were indistinguishable from motions of the liquid due to stray vibration.

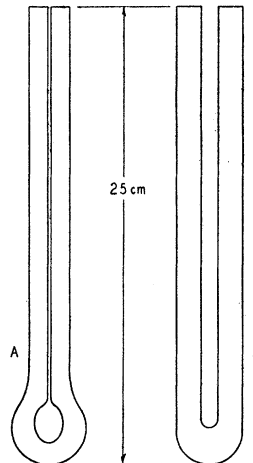


FIG. 3. Sketch of the two Pyrex U-tubes used in the experiment.

¹⁰ H. E. Hall and W. F. Vinen, *Phil. Mag.* **46**, 546 (1955).

Figure 4 shows a plot of the observations from a typical run.

Figure 4 also illustrates the method of deducing the amplitudes of the oscillations. The solid straight line is drawn to fit the final portion of the curve, where the variation of level is due to film flow and evaporation only. Assuming the oscillations have negligible effect upon film flow and evaporation, the straight line represents the mean level of the oscillating liquid; the amplitude, h , of the oscillations at a given time is thus the difference between the observed maximum level and the estimated mean level. This indirect method of finding h had to be used because it was not possible to observe minimum as well as maximum levels. In a few runs, however, rough estimates of the amplitude were made when it was less than one reticule graduation (about 0.5 mm). These made it easier to draw the straight line accurately.

To find logarithmic decrements, the values of $\log h$ were plotted against the time, t . If such a plot yields a straight line, the logarithmic decrement can be calculated from its slope and the observed period of the oscillations. In the present case, the error of the graphical construction of Fig. 4 could be as large as h itself, at the lowest amplitudes (about 50 microns). To reduce uncertainties due to the resulting scatter of the low-amplitude points, therefore, three or four separate runs were made at each temperature and combined on a single plot of $\log h$ vs t (Figs. 5 and 6). The time origins of the different runs on such a plot were adjusted to give agreement at an arbitrary ordinate (10 reticule divisions).

Figure 5 shows two plots of $\log h$ vs t for He I. In both cases the points lie close to a straight line down to the smallest amplitudes. We shall denote the reciprocal of the slope of any one of these straight lines by the symbol τ_1 . Tube B shows a deviation at very high amplitudes, which will be discussed later.

Figure 6 shows some of the results for He II. For each temperature there are two distinct ranges where

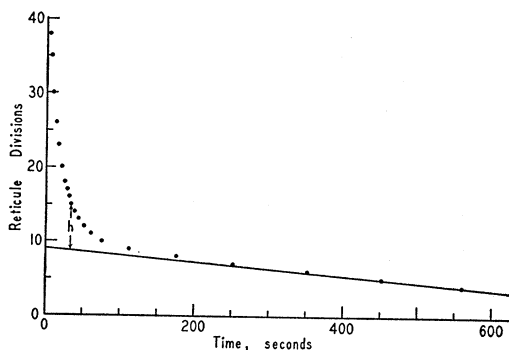


FIG. 4. Experimental values of the maximum height of the liquid in one arm of the U-tube plotted against time. The equilibrium level of the liquid has been estimated by drawing a straight line through the last two experimental points, which represent film creep and evaporation only.

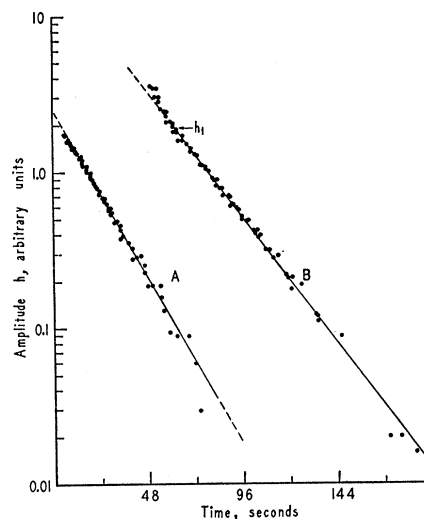


FIG. 5. Semilogarithmic plot of amplitude h (see Fig. 4) vs time t , for He I at 2.27°K. Curve A was taken from data for U-tube A. Curve B was taken from data for U-tube B and extends to higher amplitudes. At the amplitude h_i a deviation sets in, which may be due to turbulence. Each graph contains combined data from several runs. The unit of amplitude is approximately 0.53 cm.

the points lie close to straight lines. We denote the reciprocal slopes of these lines by τ_1 for the high-amplitude range and τ_2 for the low-amplitude.

Owing to the large scatter of the points, especially at small amplitudes, the following method was used to measure the slopes: five observers independently fitted straight lines to the plots of $\log h$ vs t and measured their slopes. At the same time they estimated the following "critical amplitudes": h_i , the amplitude above which the line of slope $1/\tau_1$ no longer fits the points, and (for He II only) h_n , below which this line no longer fits, and h_e , above which the line of slope $1/\tau_2$ no longer fits. Table I shows, for each set of experimental conditions, the averages of the five estimates of the quantities τ_1 , τ_2 , h_i , h_n , and h_e . The estimates varied by as much as 10% for τ_1 , 20% for τ_2 , and 50% for h_i , h_n , and h_e .

Table I also shows values for the viscosity, η_1 or η_2 , calculated from the corresponding values of τ_1 or τ_2 respectively. These were calculated using formula (16) together with the relation $\delta = P/\tau$ where P is the observed period of oscillation. In this calculation P was not measured separately for each value of τ but was given a common value for all runs with the same tube. Measurements of P at different temperatures varied only by about 1%: variations of this order of magnitude, arising from changes in δ , are to be expected theoretically. [See Eq. (A13) of the appendix.] For the suffix 1 (referring either to He I or to He II with the two fluids moving together), ρ_n/ρ was set equal to one in Eq. (16). For the suffix 2 (He II when the two-fluid equations hold), ρ_n/ρ was given the value shown in the

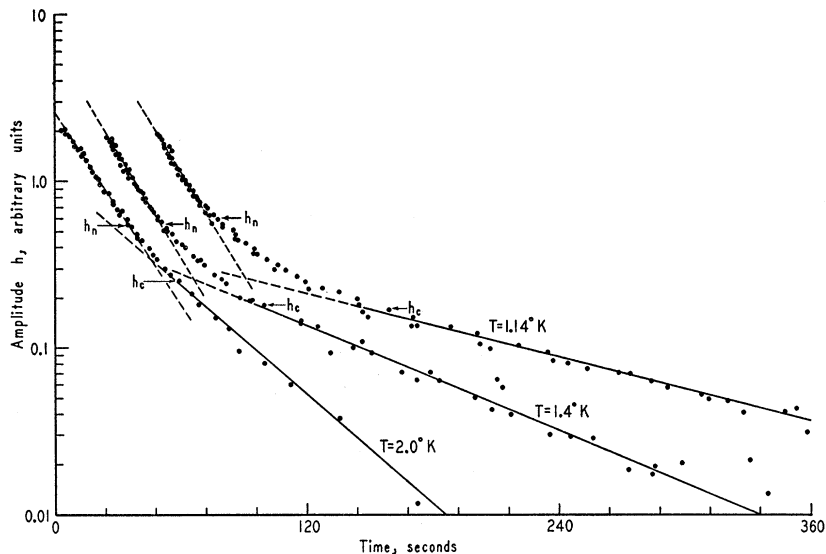


FIG. 6. Semilogarithmic plot of amplitude h vs time t for He II at three indicated temperatures. All data were taken with U-tube A . At amplitudes above h_c the two-fluid hydrodynamics is inadequate. For amplitudes between h_n and the maximum amplitude, it appears that the two fluids have identical velocity fields.

table.¹¹ For comparison, we also give values for the viscosity, interpolated from data given by Donnelly *et al.*⁸ and by Hollis Hallett.⁶ The former set of values we regard as values for η_1 , since they come from an experiment where it was shown that the normal and superfluid components moved together; the latter set, as values for η_2 , since they come from an experiment where the two-fluid hypothesis was verified by a simultaneous determination of ρ_n/ρ .

4. DISCUSSION OF THE RESULTS

Table I shows that the experiment gives values of η_1 and η_2 agreeing roughly with each other and with other experimental determinations of the viscosity. This agreement over a wide range of values of ρ_n/ρ indicates that the approximations made in Sec. 2 are not too inaccurate and supports our fundamental hypothesis that the two-fluid equations hold in the low-amplitude range and that the two fluids move together in the high-amplitude range.

Despite the poor accuracy of our values of η_1 and η_2 (the spread of the tabulated values indicates that it is about 30%), we may tentatively draw two further conclusions from them. First, we note that η_1 exceeds the corresponding value for η_2 in 10 cases out of 12, and that the geometric mean of the values of η_1/η_2 is 1.33. This indicates that the viscosity when the two fluids move as one exceeds that for the normal component alone. Secondly, the value of η_1 or η_2 obtained with tube B exceeds the corresponding values for tube A 8 times out of 9. Since the bend in tube B was sharper than that in tube A , this appears to confirm the suggestion made in Sec. 2 that a sharp bend will tend to

make the damping larger. This possibility may account for the results of a few runs using a U-tube about 1 cm in diameter with a very sharp bend. These give viscosity values as much as twice Hallett's.⁶

Although the two regions of constant damping persist to lower temperatures than in the oscillating sphere experiment, the transition does become more diffuse as the temperature is lowered (see Fig. 6), so that it is not easy to define τ_1 below 1.4°K. This broadening of the transition is reflected in the tendency of h_c to decrease as the temperature decreases, while h_n remains roughly constant (see Table I). A similar temperature dependence of the quantity corresponding to h_c was noted by Hallett⁶ for the oscillating disk experiment. We offer no explanation¹² either of the values or of the temperature dependence of h_c and h_n . Table I also indicates that h_c is greater for tube A than for tube B . Since tube B has a sharper bend, one would expect a less uniform velocity distribution over its wall, and hence, for the reasons put forward in the introduction, one might expect a less sharp transition and a lower value of h_c .

The deviation from constant damping at amplitudes exceeding h_t was observed only for tube B . This shows that the deviation was not a starting effect. No doubt the effect could have been observed with tube A too, using larger starting amplitudes. The value of h_t decreases with temperature, but is apparently unaffected

¹¹ These values were kindly supplied by A. C. Hollis Hallett who calculated them from published values for the speed of second sound and the entropy data of Kramers, Wasscher, and Gorter [Physica 18, 329 (1952)].

¹² The only quantitative description so far proposed for the breakdown of frictionless flow is that of C. J. Gorter and J. H. Mellink [Physica 15, 285 (1949)] who suggested adding nonlinear "mutual friction" terms to the two-fluid hydrodynamical equations. We were able to determine the effect of these terms only for very small amplitudes, using G. C. J. Zwanikken's method [Physica 16, 805 (1950)]. The calculation indicated that a rigorous solution of Gorter and Mellink's equations might give the right temperature dependence and order of magnitude for h_c , but it told nothing about h_n .

TABLE I. Summary of experimental results.^a

		2.27°K	2.15°K	2.00°K	1.80°K	1.60°K	1.40°K	1.20°K	1.14°K	1.05°K
ρ_n/ρ	b		0.869	0.553	0.317	0.166	0.0739	0.0282	0.0196	0.01044
τ_1 (sec)	Tube A	19.5	19.7	22.8	22.6	24.0	20.6	21.3	21.4	
τ_2 (sec)	A		22.4	39.9	46.7	67.2	86.8	97.7	137	
τ_1 (sec)	B	26.1			28.4	25.3	27.2	23.8		29.8
τ_2 (sec)	B				58.2	94.2	107	209		212
η_1 (μ poise)	A	30	29	22	22	20	27	25	25	
η_1 (μ poise)	B	35			30	38	33	43		28
η_1 (μ poise)	c	32	28	24	21	24	28	29	29	29
η_2 (μ poise)	A		26	13	16	14	18	33	24	
η_2 (μ poise)	B				22	16	26	18		38
η_2 (μ poise)	d		17.5	11.5	9.8	10.3	13.2			
h_t (cm)	B	1.2			1.15	1.23	1.01	0.80		0.85
h_n (cm)	A		0.32	0.32	0.30	0.32	0.30	0.32	0.32	
h_m (cm)	B				0.23	0.27	0.29	0.27		0.27
h_c (cm)	A		0.32	0.13	0.14	0.15	0.097	0.075	0.091	
h_c (cm)	B				0.10	0.069	0.080	0.036		0.041

^a The radius of tube A was 0.505 cm and that of B was 0.754 cm. The average observed period for tube A was $P=0.983$ sec and for B was $P=0.938$ sec.

^b See reference 11.

^c See reference 8.

^d See reference 6.

by the lambda transition. The oscillating-sphere experiment⁹ shows a very similar effect, which Benson and Hallett attribute to turbulence. They define a Reynolds number for the onset of turbulence given by the expression

$$R = \frac{(\text{maximum peripheral speed}) \times (\text{penetration depth})}{(\text{kinematic viscosity})}, \quad (19)$$

where the penetration depth is $(2\eta/\rho\omega_0)^{1/2}$ and the kinematic viscosity is η/ρ . For spheres with two different periods of oscillation they find the values 177 and 188 for R . In our case, the corresponding number is

$$R = h_t(2\omega_0\eta/\eta)^{1/2} \approx 255 \quad (20)$$

for $h_t=1$ cm, $\eta=30\mu P$. Considering the differences in the experimental arrangements and the experimental errors involved, it is probably safe to assume that the liquid is turbulent for amplitudes above h_t .

5. CONCLUSIONS

We may interpret the observed damping of oscillations of He II in a U-tube as follows. At low amplitudes the two-fluid hydrodynamical equations of motion are valid; the motion of the superfluid is irrotational. At higher amplitudes a transition takes place to a motion where the normal and superfluid components have identical velocity fields, and the motion of the superfluid is no longer irrotational. At still higher amplitudes (where the Reynolds number exceeds 255), there appears to be turbulence in He II in the classical sense.

The experiment also indicates that the viscosity coefficient when the two fluids move together is greater than when they move separately.

6. ACKNOWLEDGMENTS

We should like to thank Professor C. T. Lane, Professor Lars Onsager, and Professor G. Breit for helpful discussions, Dr. A. C. Hollis Hallett for supplying the values of ρ_n/ρ used in Table I and for permission to reproduce Fig. 1(a), and R. H. Walmsley, S. D. Elliott, Jr., and D. M. Lee for help with experimental runs and data reduction. We also gratefully acknowledge the financial support of the Office of Ordnance Research, the National Science Foundation, and the United States Educational Commission in the United Kingdom.

APPENDIX. MORE ACCURATE TREATMENT OF THE EQUATIONS OF SEC. 2

We first define a new symbol $\epsilon \equiv 1 - \omega_0/\omega$, in terms of which Eqs. (9b) and (11) become

$$z \equiv \lambda^{-1}(1 - \epsilon)^{-1/2}, \quad (A1)$$

$$-(2\epsilon - \epsilon^2)\rho / [\rho_n - (2\epsilon - \epsilon^2)\rho] = -2\lambda(1 - \epsilon)^{1/2}\phi(z), \quad (A2)$$

where

$$\phi(z) \equiv -J_1(z)/J_0(z) = J_0'(z)/J_0(z), \quad (A3)$$

the prime denoting a derivative. Rearrangement of (A2) gives

$$\frac{\epsilon\rho}{\lambda\rho_n} = \frac{(1 - \epsilon)^{1/2}}{1 - \frac{1}{2}\epsilon} \left[1 - (2\epsilon - \epsilon^2)\frac{\rho}{\rho_n} \right] \phi(z). \quad (A4)$$

In our search for an approximate solution of this equation, we use the simple approximate solution already obtained in Sec. 2 to estimate the orders of magnitude of various quantities. Equation (13) shows that $\epsilon \approx i\lambda\rho_n/\rho$ (the symbol \approx indicates equal orders of magnitude). It follows that

$$|\epsilon|^2 \leq |\epsilon|^2\rho/\rho_n \approx |\epsilon\lambda| \approx |\lambda|^2\rho_n/\rho = \eta/a^2\omega_0\rho \approx 10^{-4}. \quad (A5)$$

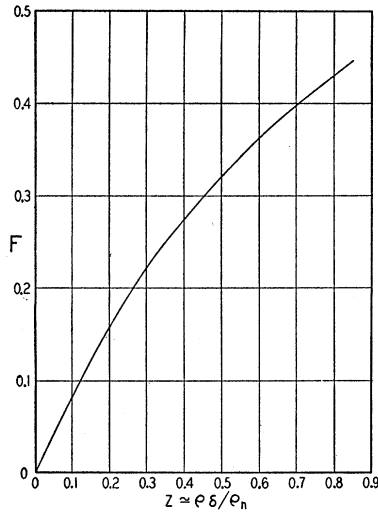


FIG. 7. The function $F(Z)$, used in calculating the viscosity from the observed damping by means of Eq. (16). For the definition of this function see the appendix.

Our approximation will be to neglect quantities $\approx 10^{-4}$. Thus Eq. (A1) becomes

$$z \simeq \lambda^{-1} (1 + \frac{1}{2}\epsilon),$$

so that

$$\phi(z) \simeq \phi(\lambda^{-1}) + \frac{1}{2}\lambda^{-1}\epsilon\phi'(\lambda^{-1}),$$

where the symbol \simeq denotes approximate equality. The asymptotic formulas for Bessel functions¹³ show that, when $\text{Im}z$ is large and negative,

$$\phi(z) = i[1 - (2iz)^{-1} + O(z^{-2})], \tag{A6}$$

so that

$$\phi'(z) = \frac{1}{2}z^{-2} + O(z^{-3}).$$

It follows that $|\phi(\lambda^{-1})| \approx 1$, that $|\lambda^{-1}\epsilon\phi'(\lambda^{-1})| \approx \frac{1}{2}|\epsilon\lambda| \ll 1$ [by (A5)], and hence that $\phi(z) \simeq \phi(\lambda^{-1})$. Substituting this into (A4), and using (A5) some more, we obtain

$$\epsilon\rho/\lambda\rho_n \simeq (1 - 2\epsilon\rho/\rho_n)\phi(\lambda^{-1}).$$

Solving this for ϵ and recalling that, by (12), $\lambda = i^{\frac{1}{2}}|\lambda|$, we obtain

$$\epsilon \simeq (\rho_n/\rho)|\lambda|[f(|\lambda|) + ig(|\lambda|)], \tag{A7}$$

where the real functions f and g are defined by

$$f + ig = [2|\lambda| + i^{-\frac{1}{2}}/\phi(\lambda^{-1})]^{-1}. \tag{A8}$$

For small $|\lambda|$, Eq. (A6) shows that

$$\begin{aligned} f &= -1/\sqrt{2} + O(\lambda^2), \\ g &= 1/\sqrt{2} + \frac{3}{2}|\lambda| + O(\lambda^2). \end{aligned} \tag{A9}$$

For larger $|\lambda|$, f or g can be evaluated numerically, by making use of the relation

$$\begin{aligned} -i^{-\frac{1}{2}}/\phi(\lambda^{-1}) &= -i^{-\frac{1}{2}}J_0(i^{-\frac{1}{2}}x)/J_0'(i^{-\frac{1}{2}}x) \\ &= iJ_0(i^{\frac{1}{2}}x)/i^{\frac{1}{2}}J_0'(i^{\frac{1}{2}}x) \\ &= i(\text{ber}x + i\text{bei}x)/(\text{ber}'x + i\text{bei}'x), \end{aligned}$$

¹³ See, for example, E. T. Copson, *The Theory of Functions of a Complex Variable* (Oxford University Press, London, 1935), pp. 335-336.

where $x \equiv |\lambda|^{-1}$, and $\text{ber}x$ and $\text{bei}x$ are the Kelvin functions. Savidge¹⁴ has tabulated the real and imaginary parts of the above expression (he calls them W/V and Z/V , respectively).

Experimentally, we measure not ϵ but the logarithmic decrement δ . According to (14) and the definition of ϵ , this is given by

$$\begin{aligned} \delta/2\pi &= [\text{Im}(1 + \epsilon + \epsilon^2 + \dots)]/[\text{Re}(1 + \epsilon + \epsilon^2 + \dots)] \\ &= [\text{Im}\epsilon + 2\text{Im}\epsilon\text{Re}\epsilon + \dots]/[1 + \text{Re}\epsilon + \dots] \\ &\simeq \text{Im}\epsilon[1 + \text{Re}\epsilon], \end{aligned} \tag{A10}$$

since $|\epsilon|^2 \ll 1$. To express $|\lambda|$ in terms of the measurable quantities δ and ρ_n/ρ , we first note that, by (A7), (A9), and (A5)

$$\text{Re}\epsilon + \text{Im}\epsilon \ll 1. \tag{A11}$$

Using (A10), (A11), and (A7), we obtain an implicit equation for $|\lambda|$:

$$\frac{\rho}{\rho_n} \frac{\delta}{2\pi} \left(1 + \frac{\delta}{2\pi}\right) \simeq \frac{\rho}{\rho_n} \text{Im}\epsilon \simeq |\lambda|g(|\lambda|). \tag{A12}$$

We shall also need an expression for ω_0 in terms of the corresponding measured quantity $2\pi/P$. Using (A11) and (A12) we find

$$2\pi/P\omega_0 = \text{Re}(1 + \epsilon + \dots) \simeq 1 - \text{Im}\epsilon \simeq 1 - \delta/2\pi. \tag{A13}$$

To express η in terms of measured quantities, we use equations (12), (A12), and (A13), together with the fact that $\delta^2 \ll 1$:

$$\begin{aligned} \eta &= \omega_0\rho na^2|\lambda|^2 \\ &\simeq (a^2\delta^2\rho^2/\pi P\rho_n)(1 + 3\delta/2\pi)(1 - F), \end{aligned} \tag{A14}$$

where $F \equiv 1 - (2g^2)^{-1}$. It is convenient to regard F as a function of $Z \equiv 2\pi|\lambda|g(|\lambda|)$ rather than of $|\lambda|$, since Z can be expressed in terms of measured quantities [Eq. (A12)]. A graph of the function $F(Z)$ is given in Fig. 7.

Equation (A9) shows that, for small $|\lambda|$,

$$\begin{aligned} 1 - F &= 1 - 3\sqrt{2}|\lambda| + O(|\lambda|^2) \\ &= 1 - 3Z/\pi + O(Z^2). \end{aligned} \tag{A15}$$

This shows, in the first place, that the approximation

$$Z \simeq \rho\delta/\rho_n, \tag{A16}$$

used in Fig. 7, is adequate for evaluating F ; for the error in F arising from this approximation is [by (A12)] roughly $(\rho\delta^2/2\pi\rho_n)dF/dZ$ and, by (A10), (A15), and (A5), this is roughly $3|\epsilon^2\rho/\rho_n| \ll 1$. Secondly, (A15) shows [together with (A5)] that $(3\delta/2\pi)F \approx 9|\epsilon\lambda| \ll 1$, so that (A14) can be replaced by our final expression for η , Eq. (16) of Sec. 2. Finally, (A15) and (A16) together give the useful approximation (17).

¹⁴ H. G. Savidge, *Phil. Mag.* **19**, 49 (1910).